

1,2-Addition versus σ -Bond Metathesis Reactions in Transient Bis(cyclopentadienyl)zirconium Imides: Evidence for a d^0 Dihydrogen Complex

Hannah E. Toomey,[†] Doris Pun,[†] Luis F. Veiros,[‡] and Paul J. Chirik^{*,†}

Department of Chemistry and Chemical Biology, Baker Laboratory, Cornell University, Ithaca, New York 14853, and Centro de Quimica Estrutural, Complexo I, Instituto Superior Técnico, Avenida Rovisco Pais 1, 1049-001 Lisbon, Portugal

Received October 18, 2007

Exposure of a series of zirconocene amido and hydrazido hydride complexes, $(\eta^5\text{-C}_5\text{Me}_4\text{H})_2\text{Zr}(\text{NHR})\text{H}$ ($\text{R} = \text{}^t\text{Bu}$, NMe_2 , Me , H), to 4 atm of D_2 gas at 56 °C produced isotopic exchange in both the N-H and Zr-H positions. In general, the relative rates of 1,2-elimination can be rationalized on the basis of ground-state effects, whereby amido compounds with the strongest N-H bonds, as judged by the corresponding free amine, undergo the slowest isotopic exchange. For the compound with the strongest N-H bond in the series, $(\eta^5\text{-C}_5\text{Me}_4\text{H})_2\text{Zr}(\text{NH}_2)\text{H}$, the barrier for 1,2-elimination is sufficiently high such that σ -bond metathesis becomes the dominant intermolecular exchange pathway. For the other amido zirconocene hydrides, the rate constants for deuterium exchange into the N-H position are faster than for the Zr-H position. This behavior is a result of a faster intramolecular isomerization process driven by an equilibrium isotope effect favoring N-D over Zr-D bond formation. Computational studies on a related model compound, $(\eta^5\text{-C}_5\text{H}_5)_2\text{Zr}(\text{NH}^t\text{Bu})\text{H}$, successfully reproduce these observations and support a pathway involving the formation of rare d^0 dihydrogen complexes.

Introduction

1,2-Addition and its microscopic reverse, 1,2-elimination, are fundamental transformations in organometallic chemistry and have found widespread application in the activation of carbon–hydrogen bonds.¹ Imido titanium and zirconium complexes, $\text{X}_2\text{Ti}=\text{NR}$ ($\text{X} = \text{amide}$, alkoxide , cyclopentadienyl), are exemplary; a range of compounds that induce C-H bond cleavage in methane and higher alkanes have been reported.^{2–4} This mechanistic paradigm has also been applied to isolobal and isoelectronic group 4 alkylidene complexes^{5,6} and more recently titanium alkylidynes.⁷ For the imido compounds, mechanistic² and computational⁸ studies support a planar, four-centered “kite-shaped” transition structure with considerable C-H bond breaking and N-H bond forming in the hydrocarbon activation step (Figure 1).

These fundamental studies in C-H activation have served as the foundation for the functionalization of coordinated

dinitrogen with nonpolar reagents. Specifically, our laboratory has reported a family of bis(cyclopentadienyl)zirconium^{9–11} and hafnium¹² compounds with strongly activated, four-electron-reduced dinitrogen ligands that exhibit significant imido character in the metal–nitrogen bonds (Figure 2).¹³ These compounds undergo the facile 1,2-addition¹⁴ of dihydrogen and C-H bonds,^{10,15} resulting in a mild method for assembly of N-H bonds in solution.

Investigations into the mechanism of N_2 hydrogenation^{10,14} and subsequent diazene dehydrogenation with an *ansa*-zirconocene complex¹¹ have relied on deuterium labeling experiments to gain insight into the 1,2-addition/elimination event. However, these studies have been complicated by competing σ -bond metathesis reactions and cyclopentadienyl substituent cyclometalation.^{16,17} In principle, the competition between 1,2-elimination and σ -bond metathesis can be delineated with an isotopic labeling study (Figure 3). The case where D_2 is added to the perprotio isotopologue is shown in Figure 3. For the extreme where 1,2-elimination/addition is exclusive, the rate of disappearance for the two positions will be equal. In the limit where σ -bond metathesis is exclusive, isotopic exchange occurs

* Corresponding author. E-mail: pc92@cornell.edu.

[†] Cornell University.

[‡] Instituto Superior Técnico.

(1) Labinger, J. A.; Bercaw, J. E. *Nature* **2002**, *417*, 507.

(2) (a) Wolczanski, P. T.; Bennett, J. L. *J. Am. Chem. Soc.* **1997**, *119*, 10696. (b) Wolczanski, P. T.; Bennett, J. L. *J. Am. Chem. Soc.* **1994**, *116*, 2179. (c) Schaller, C. P.; Cummins, C. C.; Wolczanski, P. T. *J. Am. Chem. Soc.* **1996**, *118*, 591.

(3) (a) Duncan, A. P.; Bergman, R. G. *Chem. Rev.* **2002**, *2*, 431. (b) Hoyt, H. E.; Michael, F. E.; Bergman, R. G. *J. Am. Chem. Soc.* **2004**, *126*, 1018.

(4) Hazari, N.; Mountford, P. *Acc. Chem. Res.* **2005**, *38*, 839.

(5) Mindiola, D. J. *Acc. Chem. Res.* **2006**, *39*, 813.

(6) Hanna, T. E.; Keresztes, I.; Lobkovsky, E.; Bernskoetter, W. H.; Chirik, P. J. *Organometallics* **2004**, *23*, 3448.

(7) Bailey, B. C.; Fan, H. J.; Baum, E. W.; Huffman, J. C.; Baik, M. H.; Mindiola, D. J. *J. Am. Chem. Soc.* **2005**, *127*, 16016.

(8) (a) Cundari, T. R. *Organometallics* **1993**, *12*, 1998. (b) Cundari, T. R.; Klinckman, T. R.; Wolczanski, P. T. *J. Am. Chem. Soc.* **2002**, *124*, 1481.

(9) Pool, J. A.; Lobkovsky, E.; Chirik, P. J. *Nature* **2004**, *427*, 527.

(10) Bernskoetter, W. H.; Lobkovsky, E.; Chirik, P. J. *J. Am. Chem. Soc.* **2005**, *127*, 14051.

(11) Hanna, T. E.; Keresztes, I.; Lobkovsky, E.; Chirik, P. J. *Inorg. Chem.* **2007**, *46*, 1675.

(12) Bernskoetter, W. H.; Olmos, A. V.; Lobkovsky, E.; Chirik, P. J. *Organometallics* **2006**, *25*, 1021.

(13) Chirik, P. J. *Dalton Trans.* **2007**, 16.

(14) Pool, J. A.; Bernskoetter, W. H.; Chirik, P. J. *J. Am. Chem. Soc.* **2004**, *126*, 14326.

(15) Bernskoetter, W. H.; Pool, J. A.; Lobkovsky, E.; Chirik, P. J. *J. Am. Chem. Soc.* **2005**, *127*, 7901.

(16) Thompson, M. E.; Baxter, S. M.; Bulls, A. R.; Burger, B. J.; Nolan, M. C.; Santarsiero, B. D.; Schaefer, W. P.; Bercaw, J. E. *J. Am. Chem. Soc.* **1987**, *109*, 203.

(17) Watson, P. L. *J. Am. Chem. Soc.* **1983**, *105*, 6491.

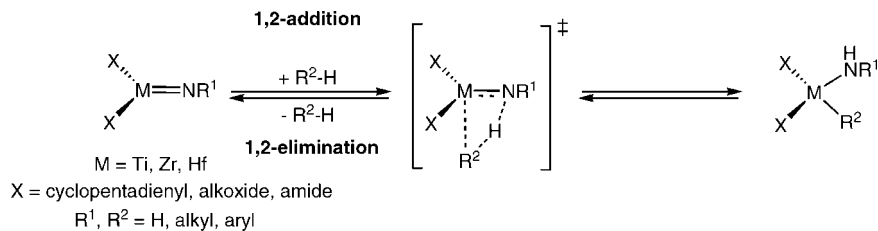


Figure 1. 1,2-Addition and elimination reactions with group 4 imido complexes and application to C–H bond activation.

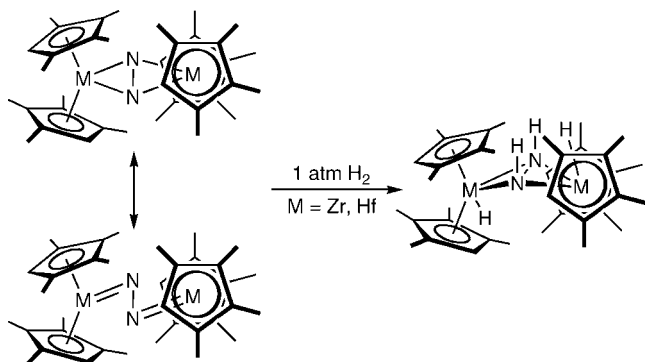


Figure 2. Application of 1,2-addition to the functionalization of coordinated dinitrogen.

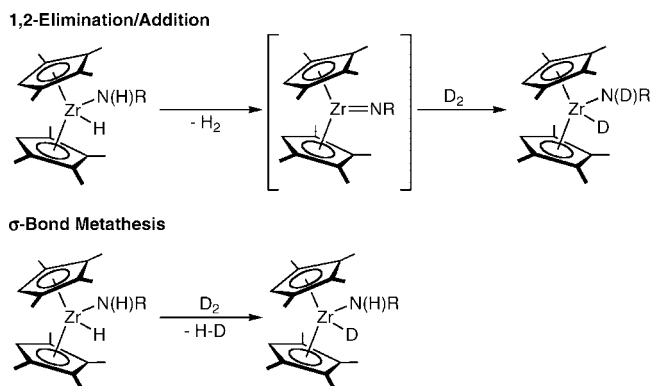


Figure 3. Isotopic exchange reactions to probe the relative rate of 1,2-addition and σ -bond metathesis reactions.

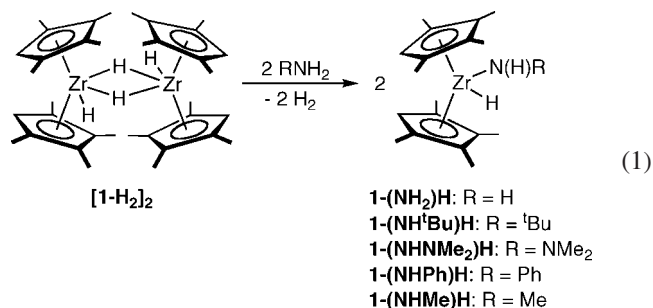
solely in the Zr–H position (Figure 3).¹⁸ Deviations from these two extremes provide the relative rates for the two competing processes.

In this study we describe a family of zirconocene amido hydride complexes, $(\eta^5\text{-C}_5\text{Me}_4\text{H})_2\text{Zr}(\text{NHR})\text{H}$ (R = H, Me, NMe₂, ^tBu, Ph), and explore the relative rate of 1,2-elimination/addition versus σ -bond metathesis as a function of amido substituent. The strength of the N–H bond in the corresponding free amine allows estimation of the rate of 1,2-elimination, while intramolecular isotopic exchange experiments augmented by computational studies have provided evidence for rare d⁰ dihydrogen complexes.

Results and Discussion

Deuterium Exchange Studies. The series of zirconocene amido hydride complexes, $(\eta^5\text{-C}_5\text{Me}_4\text{H})_2\text{Zr}(\text{NHR})\text{H}$, used in this study was prepared by addition of the appropriate primary amine

or hydrazine to $[(\eta^5\text{-C}_5\text{Me}_4\text{H})_2\text{ZrH}_2]^{19}$ (eq 1). Each compound exhibited the number of ¹H and ¹³C NMR peaks expected for a C_{3v} symmetric bent zirconocene derivative. The complete spectroscopic assignment for each compound is reported in the Experimental Section. Diagnostic N–H and Zr–H resonances were observed in the vicinity of 4.5–6.0 ppm and were assigned based on selective isotopic labeling studies (*vide infra*).



Exposure of each of the zirconocene amido hydride compounds to four atmospheres of deuterium gas at 56 °C resulted in the gradual disappearance of the N–H and Zr–H resonances. Conversions were determined by ¹H NMR spectroscopy, and the final products were assayed by ²H NMR spectroscopy to evaluate the possibility of side reactions. The *qualitative overall* rates of isotopic exchange (into both the N–H and Zr–H positions) as a function of amido substituent are presented in Figure 4. More detailed kinetic analyses will be presented later in the article.

The overall, qualitative rate of isotopic exchange correlates with the N–H bond strength of the free amine, where weaker N–H bonds correspond to faster intermolecular isotopic exchange rates. For example, zirconocene anilido hydride, **1-(NHPh)H** (BDE(N–H, PhNH₂) = 92 kcal/mol),²⁰ undergoes exchange over the course of 11 h (56 °C), while the parent zirconocene amide hydride, **1-(NH₂)H** (BDE(N–H, NH₃) = 107 kcal/mol),²¹ undergoes exchange over several weeks (56 °C).

Analysis of the deuterio isotopologues of **1-(NH₂)H**, **1-(NH^tBu)H**, and **1-(NHNMe₂)H** by ²H NMR spectroscopy following treatment with D₂ established clean isotopic exchange exclusively into the N–H and Zr–H positions, thereby ruling out competing cyclometalation processes. In contrast, the ²H NMR spectra of **1-(NHPh)H** and **1-(NHMe)H** exhibit features indicative of competing side reactions involving the amido substituent. For the anilido complex, **1-(NHPh)H**, a peak centered at 6.35 ppm, corresponding to the ortho phenyl position, was observed after 36 h at 56 °C (eq 2). By comparison, deuterium exchange in the Zr–H and N–H positions occurred over the course of

(19) Chirik, P. J.; Day, M. W.; Bercaw, J. E. *Organometallics* **1999**, *18*, 1873.

(20) Zhao, Y.; Bordwell, F. G.; Cheng, J.-P.; Wang, D. *J. Am. Chem. Soc.* **1997**, *119*, 9125.

(21) Blanksby, S. J.; Ellison, G. B. *Acc. Chem. Res.* **2003**, *36*, 255.

(18) The idealized case assumes no complication from an intramolecular 1,2-elimination event.

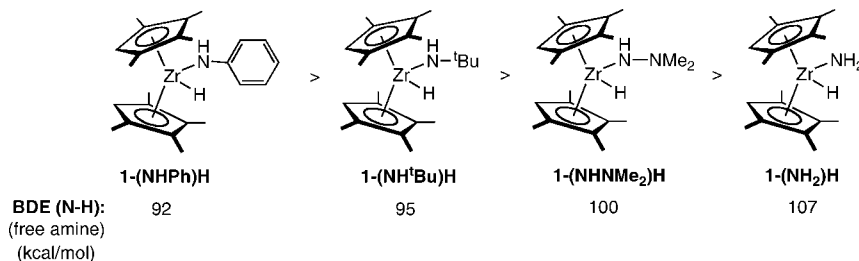
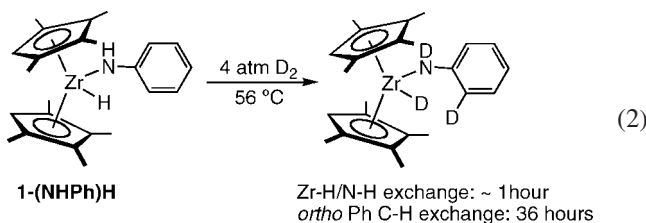
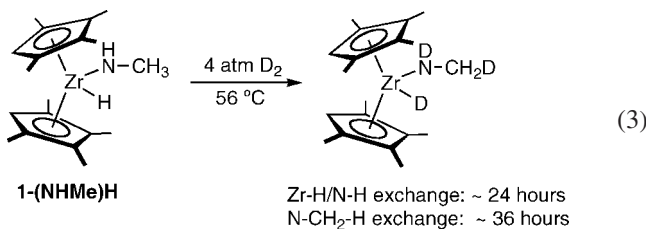


Figure 4. Relative rate of isotopic exchange into the Zr–H and N–H position as a function of amido substituent. Values for the bond dissociation of the corresponding free amine are also presented.^{20,21}

1 h at this temperature, allowing kinetic evaluation of 1,2-elimination/addition versus σ -bond metathesis (*vide infra*).



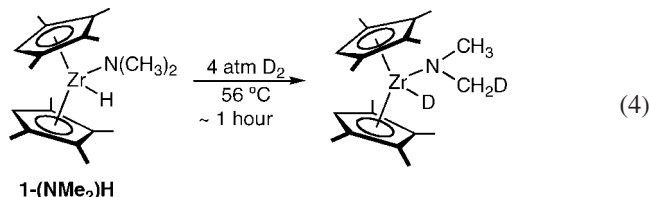
Monitoring deuterium addition to **1-(NHMe)H** by ²H NMR spectroscopy revealed a competing process that occurs on the time scale of exchange into the N–H and Zr–H positions. At 56 °C, exchange into the amido and hydride position was clearly observed after 24 h, and a new peak, centered at 3.15 ppm, appeared after 36 h. This resonance corresponds to deuterium incorporation into the amido methyl group (eq 3). Prolonged heating of the sample for 3.5 days resulted in continued deuteration of these three positions with no evidence for cyclopentadienyl group cyclometalation.



Isotopic exchange in the N–CH₃ position is consistent with metalation of the methyl substituent by either β -hydrogen elimination or σ -bond metathesis to form the zirconaaziridine intermediate. Subsequent deuteration with D₂ gas yields the experimentally observed isotopologue. Because this process occurs on the time scale of N–H and Zr–H exchange, accurate determination of the rate constants for these processes is complicated.

The scope of deuterium exchange into the methyl amido position was also explored for (η^5 -C₅Me₄H)₂Zr(NMe₂)H (**1-(NMe₂)H**). This compound was prepared in a straightforward manner by treating **1-H₂** with HNMe₂. Exposure of a benzene solution of **1-(NMe₂)H** to 4 atm of D₂ gas at 56 °C for 1 h produced isotopic exchange into the zirconium hydride position and in the amido methyl group (eq 4). While no evidence for competing cyclopentadienyl methyl group cyclometalation was obtained at this temperature, heating to 75 °C resulted in deuterium incorporation into the cyclopentadienyl methyl groups after several days.

Deuterium exchange in the amido methyl positions of **1-(NHMe)H** and **1-(NMe₂)H** most likely occurs via dihydrogen



loss and formation of a zirconaaziridine intermediate.²² For bis(cyclopentadienyl)zirconium, a number of ligand-stabilized zirconaaziridines have been prepared and are readily accessed by methane²³ or benzene²⁴ elimination from the corresponding zirconocene methyl or phenyl amide complex, respectively. Both linear free energy relationships and observation of large normal, primary kinetic isotope effects are consistent with a σ -bond metathesis process that proceeds through an ordered four-centered transition structure.²⁵ For **1-(NHMe)H** and **1-(NMe₂)H**, σ -bond metathesis to access the zirconaaziridine intermediate is likely, although β -hydrogen elimination from the amide methyl group²⁶ followed by H₂ loss cannot be ruled out on the basis of our data. Addition of D₂ gas to the zirconaaziridine accounts for the isotopic exchange process (Figure 5). A similar deuteration step from the zirconaaziridine intermediate is also likely operative for **1-(NHPH)H** and accounts for the selective isotopic exchange observed in the *ortho* position of the phenyl substituent.

For **1-(NMe₂)H** an additional process with a higher barrier is also operative. Addition of a cyclopentadienyl methyl C–H to the zirconaaziridine intermediate followed by deuterolysis also occurs and accounts for the observation of isotopic exchange in these positions at longer reaction times.

Kinetics of 1,2-Elimination/Addition versus σ -Bond Metathesis. Rate constants for the isotopic exchange of deuterium into the Zr–H and N–H positions were measured for a series of the zirconocene amido hydride compounds with the goal of gauging the relative rates of 1,2-elimination/addition versus σ -bond metathesis. Each isotopic exchange reaction was conducted at 56 °C, and conversions were determined by integrating the signals for the Zr–H and N–H position in the ¹H NMR spectra versus an internal ferrocene standard as a function of time. The first compound to be examined was **1-(NHtBu)H**. A sample plot for the disappearance of the Zr–H and N–H resonances as a function of time is presented in Figure 6.

(22) Cummings, S. A.; Tunge, J. A.; Norton, J. R. *Top. Organomet. Chem.* **2005**, *10*, 1.

(23) Buchwald, S. L.; Wanamaker, M. W.; Watson, B. T.; Dewan, J. C. *J. Am. Chem. Soc.* **1989**, *111*, 4486.

(24) Harris, M. C. J.; Whitby, R. J.; Blagg, J. *Tetrahedron Lett.* **1994**, *35*, 2431.

(25) Coles, N.; Harris, M. C. J.; Whitby, R. J.; Blagg, J. *Organometallics* **1994**, *13*, 190.

(26) Tsai, Y. C.; Johnson, M. J. A.; Mindiola, D. J.; Cummins, C. C.; Klooster, W. T.; Koetzle, T. F. *J. Am. Chem. Soc.* **1999**, *121*, 10426.

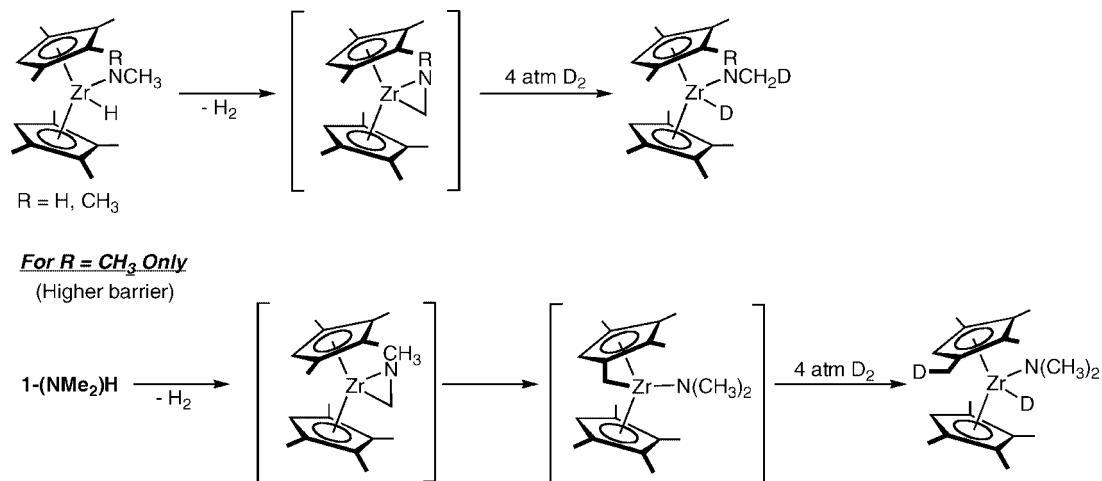


Figure 5. Proposed mechanism to account for deuterium exchange into (a) the amido methyl groups in **1-(NHMe)H** and **1-(NMe₂)H** and (b) the cyclopentadienyl methyl groups of **1-(NMe₂)H**.

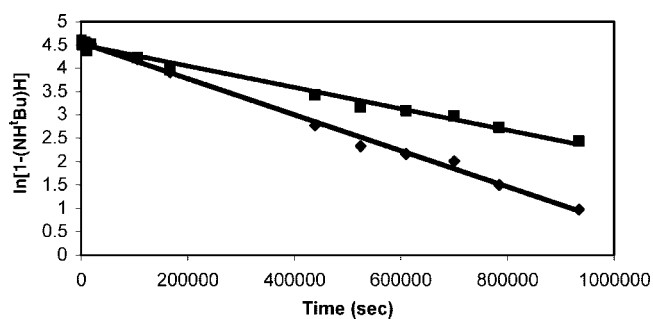


Figure 6. Sample first-order plot for deuterium incorporation in the Zr–H (boxes) and N–H (diamonds) positions of **1-(NH^tBu)H** at 56 °C.

Table 1. Rate Constants Determined at 56 °C for Isotopic Exchange into the Zr–H and N–H Positions of (η^5 -C₅Me₄)₂Zr(NHR)H Complexes

compound	$k(\text{Zr-H}) \times 10^6 \text{ s}^{-1}$	$k(\text{N-H}) \times 10^6 \text{ s}^{-1}$
1-(NH^tBu)H	1.8(4)	3.4(7)
1-(NHNMe₂)H	0.40(2)	1.1(1)
1-(NHPh)H	42.6(6)	77.7(4)
1-(NH₂)H	0.30(1)	0.16(2)

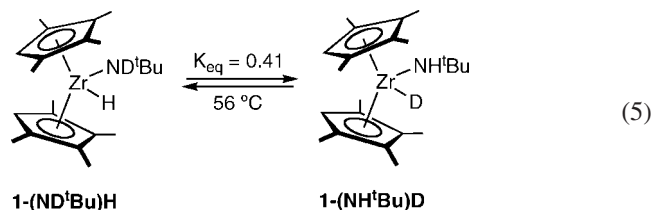
The average of three independent trials yielded observed first-order rate constants of 3.4(7) and 1.8(4) $\times 10^{-6} \text{ s}^{-1}$ at 56 °C for N–H and Zr–H disappearance, respectively. Although clean first-order behavior was obtained, the observed rate constant for isotopic exchange into the N–H position is nearly twice that for the Zr–H. Rate constants for deuterium exchange with other (η^5 -C₅Me₄)₂Zr(NHR)H complexes were also determined at 56 °C and are compiled in Table 1. With the exception of **1-(NH₂)H**, the observed rate constants for deuterium incorporation into the Zr–H position are *smaller* than those for the N–H of the amido group.

With the exception of **1-(NH₂)H**, the experimentally observed rate constants demonstrate that an *intramolecular* isotopic exchange event occurs faster than the *intermolecular* σ -bond metathesis and 1,2-elimination/addition processes presented in Figure 3. For **1-(NH₂)H** the ground-state stabilization arising from the strong N–H bond raises the barrier for 1,2-elimination and makes intermolecular σ -bond metathesis dominant over the intramolecular process.

To further explore the mechanism of the intramolecular isotopic exchange process, the preparation of mono(deutero)

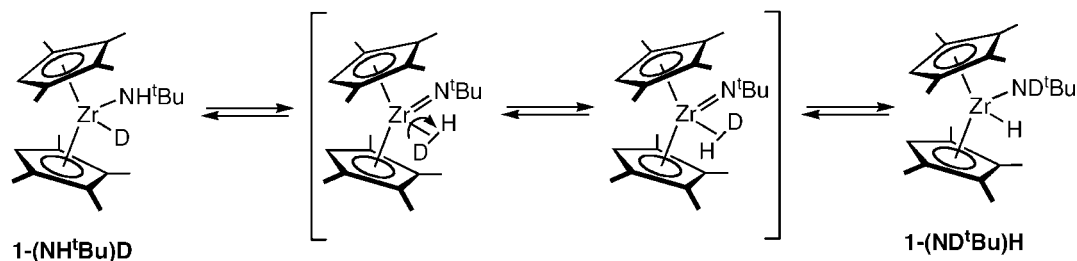
isotopologues of the *tert*-butylamido zirconocene hydride complex was targeted. The isotopologue with deuterium in the amido position, **1-(ND^tBu)H**, was synthesized by addition of ^tBuND₂²⁷ to **1-H₂**. Its isotopomer, **1-(NH^tBu)D**, was obtained by treatment of **1-D₂** with ^tBuNH₂. In the latter procedure, special care was taken to add the amine almost immediately (<1 h) after preparation of **1-D₂** to avoid complications associated with competing cyclometalation of the cyclopentadienyl methyl substituents.¹⁹ These selective labeling experiments also allowed definitive assignment of the N–H and Zr–H resonances. Isotopic exchange was not observed at ambient temperature.

With both mono(deutero) isotopomers in hand, the equilibration between them was studied at 56 °C (eq 5). Monitoring the ²H NMR spectrum of **1-(NH^tBu)D** at 56 °C demonstrated steady growth of a resonance at 5.23 ppm over the course of 4 h, corresponding to deuterium incorporation in the N–H(D) position of the amido group. In the converse experiment, warming a benzene solution of **1-(ND^tBu)H** under identical conditions also produced intramolecular isotopic exchange and yielded the same equilibrium mixture. Importantly, both isotopomers reach equilibrium *faster* than the time required for significant intermolecular deuterium incorporation, consistent with an intramolecular exchange event driven by an equilibrium isotope effect, favoring N–D over Zr–D formation, as the origin of the anomalous kinetic behavior.



Mechanistic Proposals and Computational Studies. Two mechanisms were considered for the intramolecular isotopic exchange process and are presented in Figure 7. The first pathway (Path A) begins with 1,2-elimination from **1-(NH^tBu)D** to form an imido zirconocene η^2 dihydrogen complex as an intermediate. Rotation of the η^2 H–D ligand (without dissociation) followed by 1,2-addition yields the experimentally ob-

(27) Wang, J.; Dash, A. K.; Kapon, M.; Berthet, J.-C.; Ephritikhine, M.; Eisen, M. S. *Chem.–Eur. J.* **2002**, *8*, 5384.

Path A: η^2 -Dihydrogen Complex

Path B: N-H Reductive Coupling

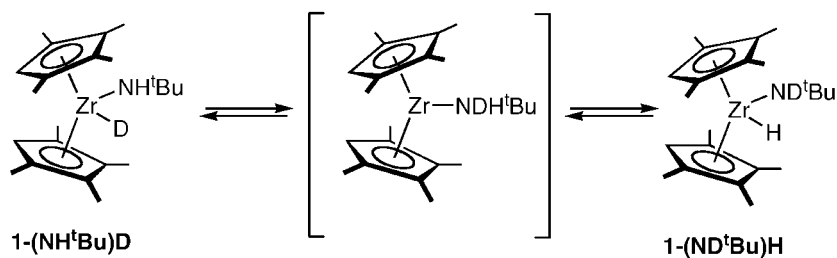


Figure 7. Proposed mechanisms for intramolecular isotopic exchange with **1-(ND^tBu)H**.

served **1-(ND^tBu)H**. In the second pathway (Path B), **1-(NH^tBu)D** undergoes reductive coupling to form a transient amine complex, which then undergoes oxidative addition to yield the observed product.

Because distinguishing these two pathways is difficult experimentally, computational studies were conducted. The model complex ($\eta^5\text{-C}_5\text{H}_5$)₂Zr(NH^tBu)H (**A**) was used for computational expediency. Free energy profiles evaluating each mechanistic possibility are presented in Figure 8.

For the 1,2-elimination pathway, an accessible barrier of 26 kcal/mol was calculated for the initial, rate-determining H₂ elimination step followed by a very shallow surface for rotation of the η^2 -dihydrogen ligand. The transition state calculated for H₂ elimination (**TS_{AB}**) is a rather late one. The formation of the H–H bond is well advanced, with a distance (0.972 Å) only 0.2 Å longer than the one in the resulting dihydrogen complex, **B**. The H–H Wiberg index (WI)²⁸ corroborates the intermediacy of an η^2 -dihydrogen complex: 0.515 in **TS_{AB}** and 0.783 in **B**. Rotation of the η^2 -dihydrogen ligand in **B** is facile, with an energy barrier of only 2 kcal/mol. In the corresponding 180° movement, the conformation of dihydrogen goes from coplanar to the metallocene wedge, in **B**, to perpendicular to this plane in the transition state, **TS_{BB}**, and finally back to planar. The third step is the microscopic reverse of the first one and regenerates the amido zirconocene hydride complex **A**.

By comparison, the alternative reductive coupling pathway proceeds with a much higher barrier of 43 kcal/mol to form the amine complex. When the transition state (**TS_{AC}**) is reached, a strong Zr–H bond persists ($d = 1.950$ Å, WI = 0.489), while the formation of the new N–H bond is well advanced ($d = 1.351$ Å, WI = 0.382). In the second step, subsequent Zr–N rotation on intermediate **C**, the amine complex, proceeds on a fairly shallow surface, with an energy barrier of only 2 kcal/mol, going through **TS_{CC}**. The final step is the microscopic

reverse of the first, regenerating the original reactant (**A**) by oxidative addition.

In summary, the results of the computational study clearly support 1,2-elimination followed by formation and rotation of an intermediate η^2 -dihydrogen complex. Thus, the observation of intramolecular isotopic exchange between **1-(ND^tBu)H** and **1-(NH^tBu)D** at 56 °C at a rate *faster* than intermolecular isotopic exchange between **1-(NH^tBu)H** and D₂ gas provides kinetic evidence for an intermediate imido zirconocene dihydrogen complex (Figure 9).

The computational studies also successfully reproduce the equilibrium isotope effect measured for the intramolecular rearrangement of **1-(ND^tBu)H** (eq 5). Recall, an experimental K_{eq} of 0.41 was measured (favoring the N–D over Zr–D isotopomer), corresponding to a difference in free energy (56 °C) of 0.6 kcal/mol. Using the model complex, ($\eta^5\text{-C}_5\text{H}_5$)₂Zr(ND^tBu)H, an equilibrium constant of 0.26 was computed, corresponding to a free energy difference of 0.9 kcal/mol.

Transition metal dihydrogen complexes, first discovered by Kubas in 1984,²⁹ are ubiquitous for d⁶ and d⁸ metal ions.³⁰ Because it is now well established that $\eta^2\text{-H}_2$ complexes are stabilized by back-donation from a filled metal orbital into the dihydrogen σ^* ,³¹ it is not surprising that d⁰ σ -complexes are rare. Computational studies have implicated $\eta^2\text{-H}_2$ intermediates in both σ -bond metathesis³² and 1,2-addition reactions^{8b,33–35} involving d⁰ group 4 transition metal compounds, although experimental evidence is limited. Ziegler has also calculated that a constrained geometry titanocene cation prefers an $\eta^2\text{-H}_2$ allyl tautomer over the olefin hydride alternative.³⁶ From these studies, the binding energy of the dihydrogen ligand has been estimated between 4 and 11 kcal/mol depending on the ancillary ligation. In the case of $\eta^2\text{-}$

(29) Kubas, G. J.; Ryan, R. R.; Swanson, B. I.; Vergamini, P. J.; Wasserman, H. J. *J. Am. Chem. Soc.* **1984**, *106*, 451.

(30) Kubas, G. J. *Metal Dihydrogen and σ -Bonded Complexes*; Kluwer: New York, 2001.

(31) Saillard, J. Y.; Hoffmann, R. *J. Am. Chem. Soc.* **1984**, *106*, 2006.

(32) Ziegler, T.; Folga, E.; Berces, A. *J. Am. Chem. Soc.* **1993**, *115*, 636.

(33) Rappe, A. K. *Organometallics* **1987**, *6*, 354.

(28) (a) Wiberg, K. B. *Tetrahedron* **1968**, *24*, 1083. (b) Wiberg indices are electronic parameters related to the electron density between atoms. They can be obtained from a natural population analysis and provide an indication of the bond strength.

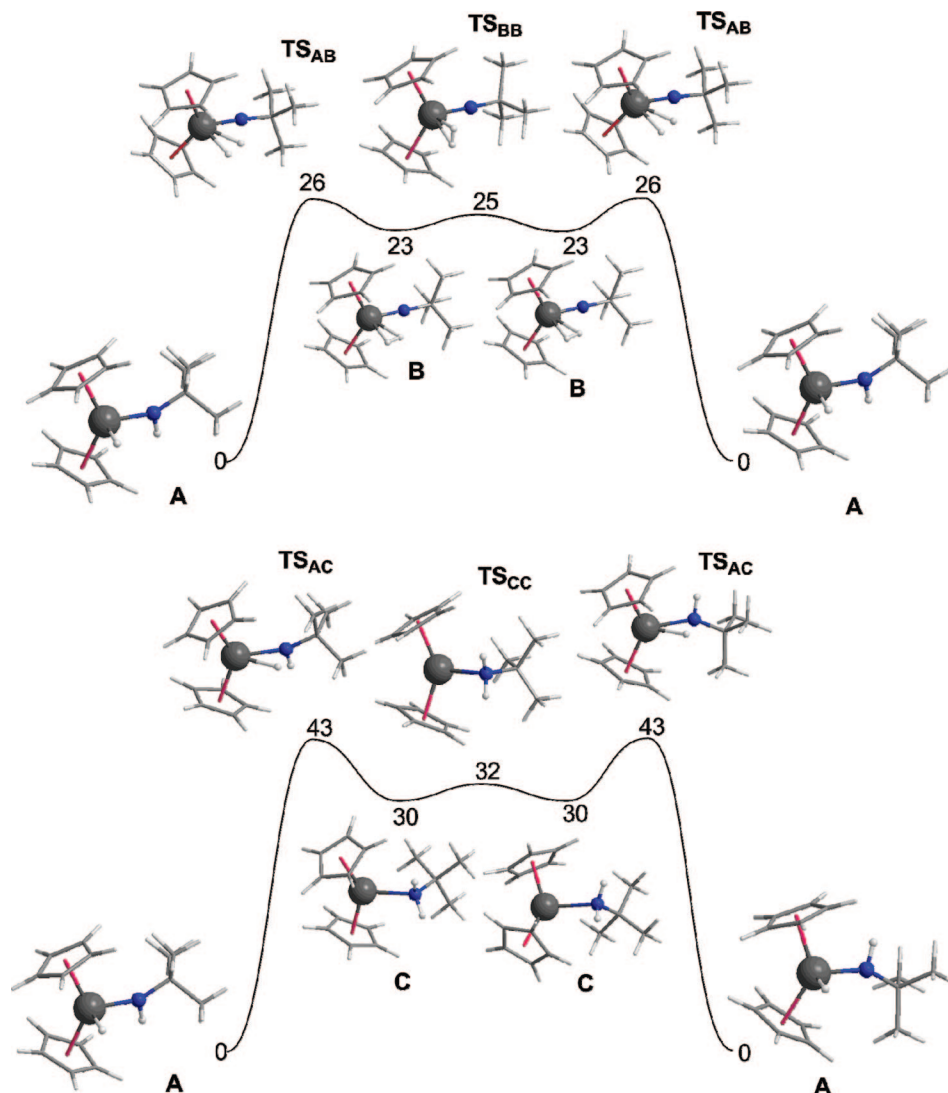


Figure 8. Free energy profiles for evaluating 1,2-elimination (top) versus reductive coupling (bottom) for intramolecular isotopic exchange for $(\eta^5\text{-C}_5\text{H}_5)_2\text{Zr}(\text{NH}^i\text{Bu})\text{H}$. **A** = $(\eta^5\text{-C}_5\text{H}_5)_2\text{Zr}(\text{NH}^i\text{Bu})\text{H}$, **B** = $(\eta^5\text{-C}_5\text{H}_5)_2\text{Zr}(\text{N}^i\text{Bu})(\eta\text{H}_2)$, **C** = $(\eta^5\text{-C}_5\text{H}_5)_2\text{ZrNH}_2^i\text{Bu}$.

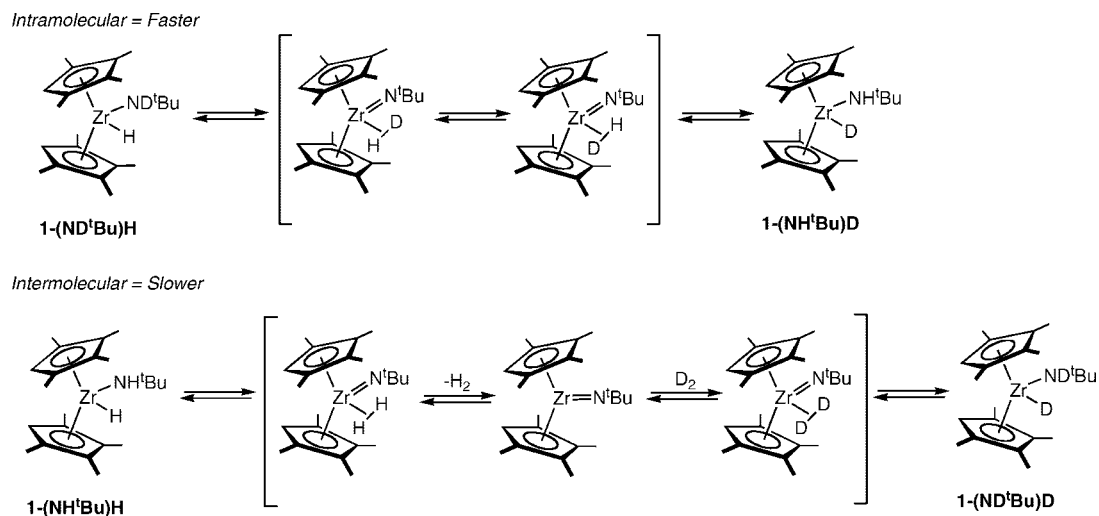


Figure 9. Proposed mechanism for intra- and intermolecular isotopic exchange with the amide hydrogen and the zirconium hydride.

H_2 in model complex **B**, a binding energy of 7.2 kcal/mol was calculated, well within the expected range.³⁷ Importantly this value is higher than that (2 kcal/mol) calculated for the 180° rotation.

The relative rates of intra- and intermolecular isotopic exchange in the zirconocene amido hydride (deuteride) complexes provide rare experimental and computational evidence for the intermediacy of a d^0 , $\eta^2\text{-H}_2$ zirconocene complex. These

results demonstrate that following 1,2-elimination, the barrier for substitution by dissociation of the η^2 -H₂ (or isotopologue) by free H₂ (or isotopologue) is higher than for rotation and readdition. To our knowledge, the only other experimental evidence for d⁰ σ -complexes has been provided by Schafer and Wolczanski, who reported that alkane compounds precede C–H activation in tungsten(VI) tris(imido) species.³⁸

Concluding Remarks

Deuterium exchange studies with a series of bis(cyclopentadienyl)zirconium amido hydride compounds have revealed a number of competing pathways. For all compounds studied, intermolecular isotopic exchange was observed in both the N–H position of the amido ligand and in the zirconium hydride. For compounds bearing anilido or methylamido substituents, competing cyclometalation, likely through a zirconaziridine intermediate, resulted in exchange into the phenyl or methyl group. In general, the rate of intermolecular isotopic exchange correlates with the N–H bond strength of the free amine, where stronger N–H bonds result in slower rates. Accordingly, the parent amido zirconocene hydride undergoes intermolecular isotopic exchange predominantly by a σ -bond metathesis pathway. In some instances, the rate constant for the Zr–H isotopic exchange was slower than that for deuterium incorporation into the N–H position. This unexpected observation is readily accommodated by a faster intramolecular process whereby 1,2-elimination produces a rare example of a d⁰ η^2 -dihydrogen complex that undergoes rotation faster than substitution. The anomalous rate constants observed for isotopic exchange are driven by an equilibrium isotope effect where the deuterium atom prefers the N–H over the Zr–H position.

Experimental Section

General Considerations. All air- and moisture-sensitive manipulations were carried out using standard high vacuum line, Schlenk, or cannula techniques or in an MBraun inert atmosphere drybox containing an atmosphere of purified dinitrogen. The MBraun drybox was equipped with a cold well designed for freezing samples in liquid nitrogen. Solvents for air- and moisture-sensitive manipulations were dried and deoxygenated using literature procedures.³⁹ Toluene, benzene, pentane, and heptane were further dried by distillation from “titanocene”.⁴⁰ Deuterated solvents for NMR spectroscopy were dried over 4 Å molecular sieves. Argon, hydrogen, and deuterium gas were purchased from Airgas Incorporated and passed through a column containing manganese oxide on vermiculite and 4 Å molecular sieves before admission to the high-vacuum line. All amines and dimethylhydrazine were purchased from Aldrich or Acros and dried over CaH₂.

(34) (a) Yates, D. F.; Basch, H.; Musaev, D. G.; Morokuma, K. *J. Chem. Theory Comp.* **2006**, *2*, 1298. (b) Bobadova-Parvanova, P.; Wang, Q. F.; Quinonero-Santiago, D.; Morokuma, K.; Musaev, D. G. *J. Am. Chem. Soc.* **2006**, *128*, 11391.

(35) Martinez, S.; Morokuma, K.; Musaev, D. G. *Organometallics* **2007**, *26*, 5978.

(36) Margl, P. M.; Woo, T. K.; Blochl, P. E.; Ziegler, T. *J. Am. Chem. Soc.* **1998**, *120*, 2174.

(37) Calculated as the difference between the energy of the dihydrogen complex (**B**) and the energy of the separated fragments: $[E\{\text{H}_2\} + E\{\text{ZrCp}_2(\text{N}^i\text{Bu})\}] - E\{\text{ZrCp}_2(\text{H}_2)(\text{N}^i\text{Bu})\}$.

(38) Schafer, D. F.; Wolczanski, P. T. *J. Am. Chem. Soc.* **1998**, *120*, 4881.

(39) Pangborn, A. B.; Giardello, M. A.; Grubbs, R. H.; Rosen, R. K.; Timmers, F. J. *Organometallics* **1996**, *15*, 1518.

(40) Marvich, R. H.; Brintzinger, H. H. *J. Am. Chem. Soc.* **1971**, *93*, 2046.

¹H NMR spectra were recorded on a Varian Inova 400 spectrometer operating at 399.799 MHz (¹H), while ²H and ¹³C spectra were collected on a Varian Inova 500 spectrometer operating at 76.7407 and 125.704 MHz, respectively. Infrared spectra were collected on a Thermo spectrometer. Elemental analyses were performed at Robertson Microlit Laboratories, Inc., in Madison, NJ.

General Procedure for Collecting Kinetic Data. The desired amido zirconocene sample was prepared from a 0.060 M stock solution in benzene-*d*₆ and transferred (0.5 mL) into a J. Young tube along with approximately 3 mg of ferrocene as an internal standard. On the high-vacuum line, the tube was degassed and 1 atm of dihydrogen was added at –196 °C. The sample was warmed to room temperature and then placed in a temperature-controlled silicon oil bath set to 56 °C. The decay of the ¹H NMR signal for the NH and ZrH peaks was monitored as a function of time versus the ferrocene standard. Rate constants for **1-(NHPh)H** were determined in the NMR probe directly at 56 °C.

Computational Details. All calculations were performed using the Gaussian 03 software package,⁴¹ and the PBE1PBE functional, without symmetry constraints. That functional uses a hybrid generalized gradient approximation (GGA), including a 25% mixture of Hartree–Fock⁴² exchange with DFT⁴³ exchange–correlation, given by the Perdew, Burke, and Ernzerhof functional (PBE).⁴⁴ The optimized geometries were obtained with the LanL2DZ basis set⁴⁵ augmented with an f-polarization function,⁴⁶ for Zr, and a standard 6-31G(d,p)⁴⁷ for the remaining elements. Transition-state optimizations were performed with the synchronous transit-guided quasi-Newton method (STQN) developed by Schlegel et al.⁴⁸ Frequency calculations were performed to confirm the nature of the stationary points, yielding one imaginary frequency for the transition states and none for the minima. Each transition state was further confirmed by following its vibrational mode downhill on both sides and obtaining the minima presented on the energy

(41) Frisch, M. J.; Trucks, G. W.; Schlegel, H. B.; Scuseria, G. E.; Robb, M. A.; Cheeseman, J. R.; Montgomery, J. A., Jr.; Vreven, T.; Kudin, K. N.; Burant, J. C.; Millam, J. M.; Iyengar, S. S.; Tomasi, J.; Barone, V.; Mennucci, B.; Cossi, M.; Scalmani, G.; Rega, N.; Petersson, G. A.; Nakatsuji, H.; Hada, M.; Ehara, M.; Toyota, K.; Fukuda, R.; Hasegawa, J.; Ishida, M.; Nakajima, T.; Honda, Y.; Kitao, O.; Nakai, H.; Klene, M.; Li, X.; Knox, J. E.; Hratchian, H. P.; Cross, J. B.; Adamo, C.; Jaramillo, J.; Gomperts, R.; Stratmann, R. E.; Yazyev, O.; Austin, A. J.; Cammi, R.; Pomelli, C.; Ochterski, J. W.; Ayala, P. Y.; Morokuma, K.; Voth, G. A.; Salvador, P.; Dannenberg, J. J.; Zakrzewski, V. G.; Dapprich, S.; Daniels, A. D.; Strain, M. C.; Farkas, O.; Malick, D. K.; Rabuck, A. D.; Raghavachari, K.; Foresman, J. B.; Ortiz, J. V.; Cui, Q.; Baboul, A. G.; Clifford, S.; Cioslowski, J.; Stefanov, B. B.; Liu, G.; Liashenko, A.; Piskorz, P.; Komaromi, I.; Martin, R. L.; Fox, D. J.; Keith, T.; Al-Laham, M. A.; Peng, C. Y.; Nanayakkara, A.; Challacombe, M.; Gill, P. M. W.; Johnson, B.; Chen, W.; Wong, M. W.; Gonzalez, C.; Pople, J. A. *Gaussian 03*, Revision C.02; Gaussian, Inc.: Wallingford, CT, 2004.

(42) Hehre, W. J.; Radom, L.; Schleyer, P. v. R.; Pople, J. A. *Ab Initio Molecular Orbital Theory*; John Wiley & Sons: New York, 1986.

(43) Parr, R. G.; Yang, W. *Density Functional Theory of Atoms and Molecules*; Oxford University Press: New York, 1989.

(44) (a) Perdew, J. P.; Burke, K.; Ernzerhof, M. *Phys. Rev. Lett.* **1997**, *78*, 1396. (b) Perdew, J. P. *Phys. Rev. B* **1986**, *33*, 8822.

(45) (a) Dunning, T. H., Jr.; Hay, P. J. *Modern Theoretical Chemistry*; Schaefer, H. F., III, Plenum: New York, 1976; Vol. 3, p 1. (b) Hay, P. J.; Wadt, W. R. *J. Chem. Phys.* **1985**, *82*, 270. (c) Wadt, W. R.; Hay, P. J. *J. Chem. Phys.* **1985**, *82*, 284. (d) Hay, P. J.; Wadt, W. R. *J. Chem. Phys.* **1985**, *82*, 2299.

(46) Ehlers, A. W.; Böhme, M.; Dapprich, S.; Gobbi, A.; Höllwarth, A.; Jonas, V.; Köhler, K. F.; Stegmann, R.; Veldkamp, A.; Frenking, G. *Chem. Phys. Lett.* **1993**, *208*, 111.

(47) (a) Ditchfield, R.; Hehre, W. J.; Pople, J. A. *J. Chem. Phys.* **1971**, *54*, 724. (b) Hehre, W. J.; Ditchfield, R.; Pople, J. A. *J. Chem. Phys.* **1972**, *56*, 2257. (c) Hariharan, P. C.; Pople, J. A. *Mol. Phys.* **1974**, *27*, 209. (d) Gordon, M. S. *Chem. Phys. Lett.* **1980**, *76*, 163. (e) Hariharan, P. C.; Pople, J. A. *Theor. Chim. Acta* **1973**, *28*, 213.

(48) (a) Peng, C.; Ayala, P. Y.; Schlegel, H. B.; Frisch, M. J. *J. Comput. Chem.* **1996**, *17*, 49. (b) Peng, C.; Schlegel, H. B. *Isr. J. Chem.* **1994**, *33*, 449.

profiles. A natural population analysis (NPA)⁴⁹ and the resulting Wiberg indices²⁸ were used to study the electronic structure and bonding of the optimized species. Free energy values for the reaction profiles (Figure 8) were obtained at 298.15 K and 1 atm by conversion of the zero point corrected electronic energies with the thermal energy corrections based on the calculated structural and vibrational frequency data. The free energy difference (and equilibrium constant) for the two isotopomers, (η^5 -C₅H₅)₂Zr(NH^tBu)D and (η^5 -C₅H₅)₂Zr(ND^tBu)H, was calculated at 329.15 K and 1 atm, by the same process.

General Method for the Preparation of (η^5 -C₅Me₄H)₂Zr-(NHR)H. A representative procedure is given for the preparation of **1-(NH^tBu)H**. A 25 mL round-bottom flask was charged with 0.100 g (0.30 mmol) of (C₅Me₄H)₂ZrH₂ and approximately 10 mL of pentane. On the high-vacuum line, the flask was degassed at -196 °C followed by addition of ^tBuNH₂ with a 100.1 mL gas bulb (0.30 mmol, 55 Torr). After stirring overnight, the solvent was removed *in vacuo*, yielding a white solid, which was recrystallized from pentane. ¹H NMR (benzene-*d*₆, 23 °C): δ 1.27 (s, 9H, ^tBu), 1.81 (s, 6H, C₅Me₄H), 1.96 (s, 6H, C₅Me₄H), 2.04 (s, 6H, C₅Me₄H), 2.18 (s, 6H, C₅Me₄H), 4.79 (s, 1H, ZrH), 5.18 (s, 1H, NH), 5.44 (s, 2H, C₅Me₄H). ¹³C{¹H} NMR (benzene-*d*₆, 23 °C): δ 12.35, 13.18, 14.32, 14.72 (CpMe), 36.22 (CMe₃), 56.75 (CMe₃), 107.99, 114.97, 116.85, 119.12, 120.20 (Cp). IR (KBr): $\nu_{\text{N-H}}$ 3328 cm⁻¹.

Characterization Data for 1-(NHPh)H. ¹H NMR (benzene-*d*₆, 23 °C): δ 1.72 (s, 6H, C₅Me₄H), 1.85 (s, 6H, C₅Me₄H), 2.02 (s, 6H, C₅Me₄H), 2.06 (s, 6H, C₅Me₄H), 5.21 (s, 2H, C₅Me₄H), 5.77 (s, 1H, NH), 5.87 (s, 1H, ZrH), 6.82 (m, 3H, Ph), 7.15 (m, 2H, Ph). ¹³C{¹H} NMR (benzene-*d*₆, 23 °C): δ 11.91, 13.48, 14.21, 14.29 (CpMe), 108.52, 117.01, 117.69, 120.04 (Cp), 121.47 (Ph), 121.64 (Cp), 129.20, 156.72 (Ph). IR (KBr): $\nu_{\text{N-H}}$ 3340 cm⁻¹. Anal. Calcd for C₂₄H₃₃N₁Zr₁: C, 67.55; H, 7.79; N, 3.28. Found: C, 67.14; H, 7.57; N, 2.90.

Characterization Data for 1-(NHNMe₂)H. ¹H NMR (benzene-*d*₆, 23 °C): δ 1.92 (s, 6H, C₅Me₄H), 2.03 (s, 6H, C₅Me₄H), 2.09 (s,

6H, C₅Me₄H), 2.23 (s, 6H, C₅Me₄H), 4.79 (s, 1H, ZrH), 5.27 (s, 2H, C₅Me₄H), 5.34 (s, 1H, NH). ¹³C{¹H} NMR (benzene-*d*₆, 23 °C): δ 11.45, 12.56, 13.57, 13.94 (CpMe), 54.58 (NMe), 108.52, 114.78, 115.51, 119.19, 119.54 (Cp). IR (KBr): $\nu_{\text{N-H}}$ 3178 cm⁻¹. Anal. Calcd for C₂₀H₃₄N₂Zr₁: C, 61.01; H, 8.70; N, 7.11. Found: C, 60.97; H, 8.45; N, 7.39.

Characterization Data for 1-(NHMe)H. ¹H NMR (benzene-*d*₆, 23 °C): δ 1.84 (s, 6H, C₅Me₄H), 2.01 (s, 6H, C₅Me₄H), 2.05 (s, 12H, C₅Me₄H), 3.20 (d, 3H, NMe₂), 4.70 (s, 1H, ZrH), 4.90 (d, 1H, NH), 5.14 (s, 2H, CpH). ¹³C{¹H} NMR (benzene-*d*₆, 23 °C): δ 12.08, 13.23, 14.12, 14.39 (CpMe), 41.67 (NMe), 108.38, 115.17, 115.52, 119.72, 119.91 (Cp). This compound was isolated as a thick oil, precluding combustion analysis.

Characterization Data for 1-(NH₂)H. ¹H NMR (benzene-*d*₆, 23 °C): δ 1.83 (s, 6H, C₅Me₄H), 1.87 (s, 6H, C₅Me₄H), 2.03 (s, 6H, C₅Me₄H), 2.14 (s, 6H, C₅Me₄H), 4.20 (s, 2H, NH₂), 4.85 (s, 1H, ZrH), 5.02 (s, 2H, C₅Me₄H). ¹³C{¹H} NMR (benzene-*d*₆, 23 °C): δ 11.79, 13.38, 13.75, 15.06 (CpMe), 106.10, 114.35, 116.42, 119.68, 121.19 (Cp). IR (KBr): $\nu_{\text{N-H}}$ 3429, 3353 cm⁻¹. Anal. Calcd for C₁₈H₂₉N₁Zr₁: C, 61.65; H, 8.34; N, 3.99. Found: C, 61.74; H, 8.54; N, 3.86.

Characterization Data for 1-(NMe₂)H. ¹H NMR (benzene-*d*₆, 23 °C): δ 1.86 (s, 6H, C₅Me₄H), 2.01 (s, 6H, C₅Me₄H), 2.04 (s, 6H, C₅Me₄H), 2.11 (s, 6H, C₅Me₄H), 2.58 (s, 6H, NMe₂), 5.05 (s, 2H, CpH), 5.88 (s, 1H, ZrH). ¹³C{¹H} NMR (benzene-*d*₆, 23 °C): δ 12.05, 13.42, 13.49, 14.71 (CpMe), 40.79 (NMe), 108.74, 113.81, 116.69, 120.34, 124.63 (Cp). This compound was isolated as a thick oil, precluding combustion analysis.

Acknowledgment. We thank the Department of Energy, Office of Basic Energy Sciences (DE-FG02-05-ER659), for financial support. P.J.C. is a Cottrell Scholar sponsored by the Research Corporation, a David and Lucille Packard Fellow in Science and Engineering, and a Camille Dreyfus Teacher-Scholar.

Supporting Information Available: Select kinetic data, representative ¹H NMR spectra of **1-(NMe₂)H** and **1-(NHMe)H**, and coordinates of all computationally optimized structures in PDF format. This material is available free of charge via the Internet at <http://pubs.acs.org>.

OM7010485

(49) (a) Carpenter, J. E.; Weinhold, F. *J. Mol. Struct. (THEOCHEM)* **1988**, *169*, 41. (b) Carpenter, J. E. Ph.D. Thesis, University of Wisconsin, Madison, WI, 1987. (c) Foster, J. P.; Weinhold, F. *J. Am. Chem. Soc.* **1980**, *102*, 7211. (d) Reed, A. E.; Weinhold, F. *J. Chem. Phys.* **1983**, *78*, 4066. (e) Reed, A. E.; Weinhold, F. *J. Chem. Phys.* **1983**, *78*, 1736. (f) Reed, A. E.; Weinstock, R. B.; Weinhold, F. *J. Chem. Phys.* **1985**, *83*, 735. (g) Reed, A. E.; Curtiss, L. A.; Weinhold, F. *Chem. Rev.* **1988**, *88*, 899. (h) Weinhold, F.; Carpenter, J. E. *The Structure of Small Molecules and Ions*; Plenum: New York, 1988; p 227.